JOURNAL OF VIROLOGY, Aug. 2005, p. 9756–9764 Vol. 79, No. 15
0022-538X/05/$08.00+0 doi:10.1128/JVI.79.15.9756–9764.2005

The Capsid Protein of Satellite Panicum Mosaic Virus Contributes to Systemic Invasion and Interacts with Its Helper Virus

Rustem T. Omarov, Dong Qi, and Karen-Beth G. Scholthof*

Department of Plant Pathology and Microbiology, Texas A&M University, College Station, Texas 77843-2132

Received 24 January 2005/Accepted 16 April 2005

Satellite panicum mosaic virus (SPMV) depends on its helper *Panicum mosaic virus* (PMV) for replication and spread in host plants. The SPMV RNA encodes a 17-kDa capsid protein (CP) that is essential for formation of its 16-nm virions. The results of this study indicate that in addition to the expression of the full-length SPMV CP from the 5′-proximal AUG start codon, SPMV RNA also expresses a 9.4-kDa C-terminal protein from the third in-frame start codon. Differences in solubility between the full-length protein and its C-terminal product were observed. Subcellular fractionation of infected plant tissues showed that SPMV CP accumulates in the cytosol, cell wall-, and membrane-enriched fractions. However, the 9.4-kDa protein exclusively cofractionated with cell wall- and membrane-enriched fractions. Earlier studies revealed that the 5′-untranslated region (5′-UTR) from nucleotides 63 to 104 was associated with systemic infection in a host-specific manner in millet plants. This study shows that nucleotide deletions and insertions in the 5′-UTR plus simultaneous truncation of the N-terminal part of the CP impaired SPMV spread in foxtail millet, but not in proso millet plants. In contrast, the expression of the full-length version of SPMV CP efficiently compensated the negative effect of the 5′-UTR deletions in foxtail millet. Finally, immunoprecipitation assays revealed the presence of a specific interaction between the capsid proteins of SPMV and its helper virus (PMV). Our findings show that the SPMV CP has several biological functions, including facilitating efficient satellite virus infection and movement in millet plants.

Satellite viruses and satellite nucleic acids (satellite RNAs and satellite DNAs) represent a group of subviral nucleic acid molecules that require a helper virus for replication and movement (30, 31). Satellite viruses differ from satellite RNAs and satellite DNAs in their capacity to direct translation of a cognate coat protein (capsid protein [CP]), a structural component required for RNA packaging via virion assembly. Satellite viruses do not share significant sequence similarity with their helper virus. However, specific recognition by the helper virus-encoded proteins, such as the replicase and movement proteins, necessarily dictates the involvement of *cis*-acting elements on satellite virus RNA; secondary structures are possibly responsible for such interactions. To date, four satellite viruses have been characterized in plants in pair-specific relationships with a helper virus (8, 30, 31). A satellite virus in an invertebrate host has recently been reported as a coinfection with the virus of *Macrobrachium rosenbergii*, a nodavirus (36).

Satellite panicum mosaic virus (SPMV) is completely dependent on its helper *Panicum mosaic virus* (PMV) (genus *Panicovirus*; family *Tombusviridae*) for replication as well as local and systemic spread in plants (29, 33, 34). There is no significant sequence similarity between SPMV and PMV (34). PMV virions encapsidate the positive-sense, single-stranded genomic RNA (3, 19). The 4,326-nucleotide (nt) genomic RNA encodes six open reading frames (33, 34) and is the template for expression of the p48 and p112 proteins, both of which are necessary for PMV and SPMV replication (2). The 26-kDa CP and three smaller proteins (p6.6, p8, and p15) are translated from a polycistronic subgenomic RNA. These proteins have been functionally implicated in local and systemic translocation of PMV (33). Mixed infections of PMV and SPMV are synergistic, inducing severe symptoms on millet plants, including stunting and failure to set seed (29).

A 17-kDa CP is expressed from the 824-nt plus-sense, single-stranded SPMV RNA (3, 19). The CP is used to assemble 16-nm spherical satellite virus particles (19, 21). As expected, SPMV CP has a high affinity for binding SPMV RNA, as shown by gel mobility shift assays (6). In addition to RNA encapsidation, the SPMV CP is implicated in exacerbation of symptoms in millet plants (23, 24, 29). The capsid protein also elicits symptoms on a nonhost plant, *Nicotiana benthamiana* (22), a feature that may be related to the unconventional role of SPMV CP in regulating a suppressor of gene silencing (22). SPMV CP is not essential for replication and systemic movement of the satellite virus RNA in millet plants (21). However, the absence of CP expression stimulated the accumulation of SPMV-defective interfering RNAs, suggesting an additional role of the CP in maintaining SPMV RNA integrity (24).

Several *cis*-active elements on the SPMV RNA are required for SPMV replication and capsid protein translation (21). In particular, nt 63 to 104 on the 5′-untranslated region (UTR) were associated with host-specific spread of the SPMV. However, deletion of this segment also abolished wild-type CP expression (21). The aim of this study was to investigate translation of the SPMV CP gene and to dissect the contribution of the CP and the 5′-UTR in SPMV infection.

We determined that 5′-UTR deletions had host-specific effects on movement, but these effects could be neutralized by the presence of the full-length 17-kDa SPMV CP. The results also showed that the SPMV RNA can direct the translation of

* Corresponding author. Mailing address: Department of Plant Pathology and Microbiology, Texas A&M University, College Station, TX 77843-2132. Phone: (979) 845-8265. Fax: (979) 845-6483. E-mail: kbgs@tamu.edu.

a 9.4-kDa protein that initiates translation downstream and in frame with the authentic SPMV CP start codon. Subcellular fractionation of infected plant tissues showed that the 17-kDa CP accumulated in the cytosol, presumably the site of virion assembly, as well as with the cell wall- and membrane-enriched fractions. In contrast, the 9.4-kDa protein was exclusively found in cell wall- and membrane-enriched fractions. The CP was also shown to have the novel capacity for specific interaction with the helper virus capsid protein. The collective results indicate that the unique properties of SPMV CP facilitate and enhance satellite virus viability, including its spread and accumulation.

MATERIALS AND METHODS

Plants. Proso millet (*Panicum miliaceum* cv. "Sunup") and foxtail millet (*Setaria italica* cv. "German R") were grown in the greenhouse (30°C) or growth chamber (28°C, 14 h of light; 24°C, 10 h of dark). Typically, four millet plants at the three-leaf stage were mechanically rub inoculated by mixing equal volumes of uncapped RNA transcripts (~5 μg) and RNA inoculation buffer (34).

In vitro transcription and in vitro translation. To obtain linearized DNA templates for in vitro transcription reactions, purified plasmids containing full-length PMV cDNA were digested with EcoICR1, and plasmids carrying SPMV or mutagenized SPMV cDNAs were digested with BglII. In vitro transcription reactions were conducted as previously described (23).

In vitro translation was carried out using the TnT-coupled system (Promega, Madison, WI) using wheat germ extract or rabbit reticulocyte lysate according to the manufacturer's instructions.

In planta [^{35}S]methionine protein labeling. Two weeks after germination, proso millet seedlings were rub-inoculated with a mixture of PMV and SPMV transcripts. At 5 days postinoculation (dpi) the plants were transferred to distilled water containing ~0.5 mCi of [^{35}S]methionine (Amersham, Piscataway, NJ). After 6 days of incubation in the presence of [^{35}S]methionine total proteins were isolated from the millet leaves and the extracts were subjected to immunoprecipitation as described below.

Immunoprecipitation. Immediately after harvesting, 1 g of leaf tissue was quick-frozen in liquid nitrogen and pulverized with a pestle in a mortar with 1.5 ml of ice-cold extraction medium {150 mM HEPES (pH 7.5), 0.5% Triton X-100, 0.2% 3-[(3-cholamidopropyl)-dimethylammonio]-1-propanesulfonate, 150 mM NaCl, 1 mM EDTA, 2 mM dithiothreitol (DTT)} and a protease inhibitor cocktail (Roche Diagnostics, Indianapolis, IN). The homogenized plant material was centrifuged at 10,000 × *g* at 4°C for 15 min. The resulting supernatant was used for immunoprecipitation.

A volume of 800 μl of the extract was mixed with 2 μl of PMV CP- or SPMV CP-specific rabbit polyclonal antibodies (34) and rotated for 2 h at 4°C, followed by the addition of 30 μl ImmunoPure immobilized protein G agarose beads (Pierce, Rockford, IL). The samples were then incubated at room temperature for 2 h. The beads were washed six times with ice-cold extraction buffer, and the immunoprecipitated material was separated on sodium dodecyl sulfate–12% polyacrylamide gels by electrophoresis (SDS-PAGE) followed by autoradiography or/and Western blotting.

The specificity of anti-SPMV antiserum was verified by immunoprecipitation of [^{35}S]methionine-labeled capsid protein that was synthesized by in vitro translation of full-length SPMV transcripts. As a negative control for immunoprecipitation, preimmune antiserum was used for the pull-down assay. To suppress irrelevant background signals caused mainly by cross-reaction between primary and secondary antibodies after the pull-down assay, preconjugated primary and secondary antibodies were used to probe immunoblots after immunoprecipitation (16).

Western blot assays. Protein samples were separated by SDS-PAGE in 15% polyacrylamide gels and transferred to nitrocellulose membranes (Osmonics, Westborough, MA). After transfer, the membranes were stained with Ponceau S (Sigma, St. Louis, MO) to verify protein transfer efficiency. The SPMV CP antibodies and PMV CP antibodies were diluted 1:2,000 and 1:5,000, respectively. Alkaline phosphatase conjugated to goat anti-rabbit antiserum (Sigma) was used as a secondary antibody at a dilution of 1:1,000. The immune complexes were visualized by hydrolysis of tetrazolium-5-bromo-4-chloro-3-indolyl phosphate as the substrate.

Site-directed mutagenesis. A QuikChange kit (Stratagene, La Jolla, CA) was ued for site-directed mutagenesis. SPMV/U-91 was generated by single-base insertion of uracil (U) (thymidine [T] in cDNA clone) immediately downstream of the first SPMV CP start codon at position nt 88 on the SPMV cDNA. SPMV/U-301 was derived from the SPMV/U-91 mutant with an additional insertion of uracil (U) (thymidine [T] in cDNA clone) immediately after the AUG codon at position 297. The SPMV-AUC mutant with substitution of the authentic AUG start codon at nucleotide 88 to an AUC codon was previously described (24). The SPMV/UAA-234 mutant was constructed by replacing six nucleotides immediately upstream of the second AUG (underlined; nt 235), changing the SPMV sequence from 5′-AAGGGGAUG-3′ to 5′-UGAUAAAUG-3′. All mutations were confirmed by sequencing the entire SPMV cDNA.

Construction of SPMV deletion mutants. Internal sequences from full-length SPMV cDNA clones were excised with selected restriction enzymes in various combinations, followed by Klenow treatment and ligation. Mutants SPMV/ΔSpeI-BamHI and SPMV/AUC/ΔSpeI-BamHI were generated by digestion of the full-length SPMV or SPMV/AUC cDNAs with SpeI and BamHI, respectively (Fig. 1A). Construct SPMV/ΔBsmI-MscI was obtained by digestion of the full-length SPMV cDNA with BsmI and MscI (Fig. 1A). The insertion of a ClaI restriction site was performed by digestion with BamHI followed by a fill-in reaction with Klenow fragment for constructs SPMV/insertClaI and SPMV/AUC/insertClaI. All constructs were verified by sequencing the entire SPMV cDNA.

RNA analyses. Total RNAs from 100 mg of inoculated or systemically infected leaves of millet plants were extracted at 14 dpi. The samples were pulverized in 1 ml of ice-cold extraction buffer (100 mM Tris-HCl [pH 8.0], 1 mM ETDA, 0.1 M NaCl, and 1% SDS) and extracted twice with phenol-chloroform (1:1, vol/vol) at room temperature. Total RNA was precipitated with 8 M lithium chloride (1:1, vol/vol) at 4°C for 1 h. The resulting pellets were washed with 70% ethanol, resuspended in RNase-free distilled water, and used for Northern blot hybridization. Approximately 10 μg of total plant RNA was electrophoretically separated in 1% agarose gels and transferred to nylon membranes (Osmonics, Westborough, MA). PMV and SPMV RNAs were detected by hybridization with [^{32}P]dCTP-labeled PMV- and SPMV-specific probes, respectively (34).

RESULTS

SPMV RNA directs synthesis of an alternative downstream in-frame translated version of CP. Immunoblot assays of proso and foxtail millet plants coinfected with PMV+SPMV and in vitro translation assays of SPMV RNA typically include several SPMV CP-specific bands smaller than the full-length product (Fig. 1). This observation was particularly evident when leaf extracts of infected foxtail millet plants were subjected to SDS-PAGE followed by immunoblot assays. The addition of protease inhibitor cocktail to the extraction solution did not prevent the detection of smaller protein bands extracted from PMV+SPMV-infected leaf tissue (data not shown). The presence of four in-frame start codons on the SPMV CP sequence, at nt 88 (denoted as AUG1), nt 235 (AUG2), nt 297 (AUG3), and nt 364 (AUG4) (Fig. 1A), raised the possibility that the lower-molecular-mass proteins might be authentic SPMV CP translation products.

To examine if the shortened N-terminal-truncated versions of CP were expressed by the mechanism of ribosome leaky scanning (13), full-length wild-type SPMV transcripts were translated in vitro and labeled with [^{35}S]methionine (Fig. 1B). Three proteins were detected (Fig. 1B), and immunoprecipitation with antiserum specific to SPMV CP verified that they represented CP products (data not shown). The amount of the translated product from AUG2 was considerably lower in comparison with initiation of protein translation from the downstream-positioned AUG3 codon (Fig. 1B). The absence of translation from AUG4 is most likely due to its relatively distant location from the 5′ end of SPMV RNA.

To obtain additional evidence that translation can initiate from the downstream start codons AUG2 and AUG3 (Fig. 1A), we suppressed the translational initiation of full-length

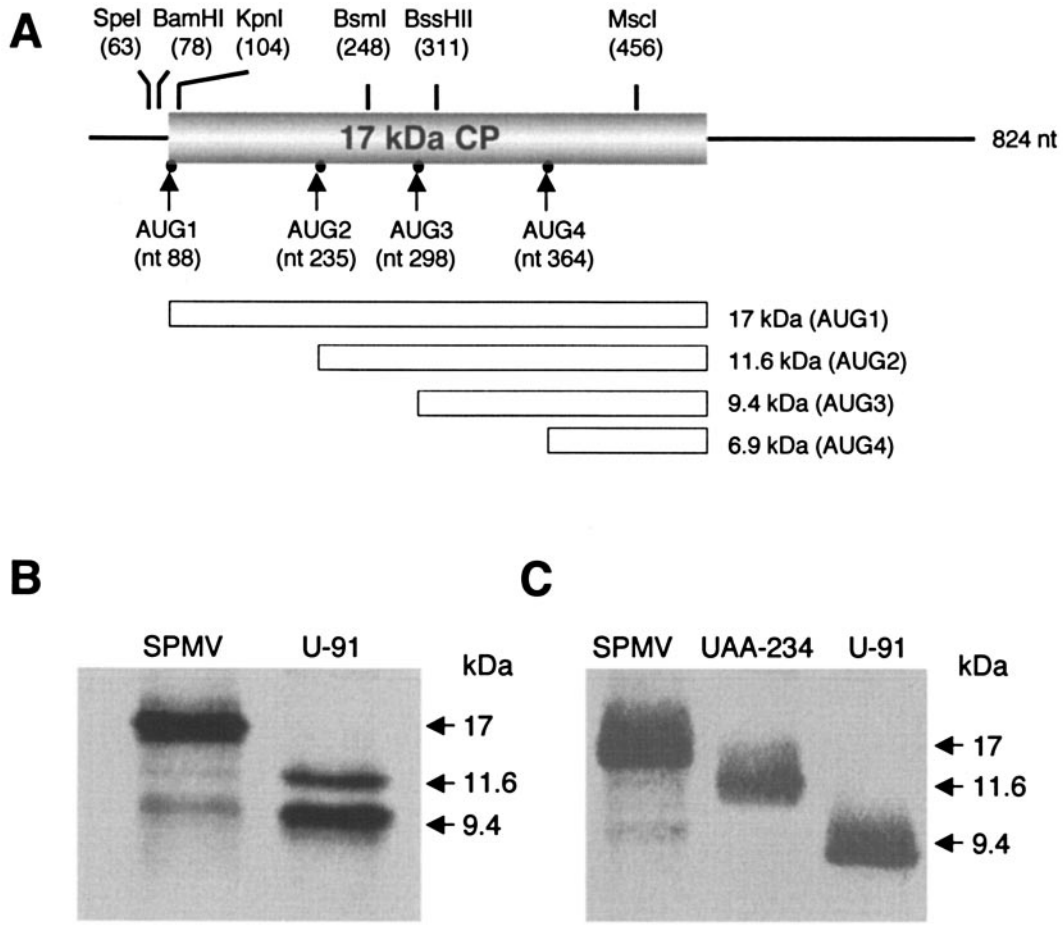

FIG. 1. SPMV genome and expression of CP. (A) Schematic representation of the 824-nt SPMV RNA (solid line) and the full-length 17-kDa CP. The restriction enzyme sites used to assemble the cDNA constructs and the positions of the predicted in-frame start codons (arrows) are indicated. The 17-kDa CP (AUG1) and N-terminal-truncated open reading frames (AUG2 to AUG4) are indicated by white rectangles. (B) In vitro translation products labeled with [^{35}S]methionine were generated from infectious transcripts of SPMV wild type and SPMV/U-91. (C) Western blot analyses of SPMV CP products in millet plants coinfected with the helper virus and the wild type (SPMV) or its mutants (UAA-234 and U-91) probed with anti-SPMV CP polyclonal antiserum. Arrows indicate the SPMV CP-specific proteins and their molecular masses.

SPMV CP from AUG1. For this purpose, a frameshift mutation was introduced by insertion of a uracil (U) (thymidine [T] in cDNA clone) immediately after AUG1 at position nt 91 (SPMV/U-91 mutant), resulting in the generation of a stop codon at position nt 96. This resulted in efficient initiation of translation from AUG2 and an even higher level of translation from the AUG3 codon, likely by leaky scanning (Fig. 1B). SPMV/U-91 transcripts were infectious, and in proso millet a 9.4-kDa truncated CP corresponding to translation initiation from AUG3 was detected (Fig. 1C). The migration of CP products produced in vitro and in vivo was also verified by mixing in vitro-translated products with extracts from infected plants, followed by SDS-PAGE and immunoblot detection (not shown).

The protein predicted to be expressed from AUG2 was not detected in PMV- plus SPMV/U-91-infected proso millet plants (Fig. 1C). The G-rich region surrounding AUG2 (GG GGAUGGGGG) might prevent or interfere with translational initiation from this codon in vivo. To test this, we replaced the authentic sequence (5′-AAGGGGAUG-3′) immediately upstream of AUG2 (underlined) with 5′-UGAUAAAUG-3′ (SPMV/UAA-234 mutant). SDS-PAGE followed by Western blotting revealed the presence of an N-terminal-truncated version of the ~12-kDa SPMV CP in infected proso millet plants (Fig. 1C). Interestingly, the immunoblot did not reveal the presence of the 9.4-kDa protein, and infected plants did not develop severe mosaic (not shown). These data indicate that preferential initiation of translation that occurred from AUG3, compared to AUG2, is most likely due to the unfavorable context surrounding AUG2. In vitro translation of capped and uncapped SPMV transcripts demonstrated identical patterns of protein synthesis in rabbit reticulocyte lysate and wheat germ extract (data not shown).

Differences in solubility and subcellular localization between full-length and the N-terminal-truncated version of CP. The extraction of CP from PMV+SPMV-infected plants under native and denaturing conditions enables reliable detection of the SPMV 17-kDa protein by Western blot analysis. The 9.4-kDa protein expressed by SPMV/U-91 was not detected under native conditions (Fig. 2), but the addition of 2% Triton X-100 to the extraction buffer allowed for its solubilization. The application of an anionic detergent (1% SDS) to the extraction

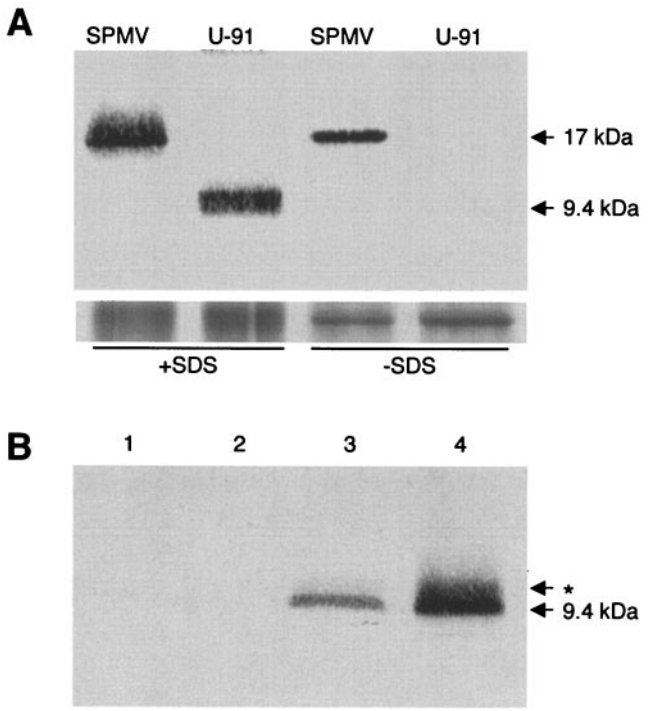

FIG. 2. Differences in solubility of the 17-kDa SPMV CP and the 9.4-kDa N-terminally truncated SPMV/U-91 CP isolated from millet plants coinoculated with *Panicum mosaic virus*. (A) Extraction and immunoblot detection of the capsid protein from SPMV and SPMV/U-91 under native (–SDS) and denaturing (+SDS) conditions. The lower panel represents a gel stained with Coomassie brilliant blue R to verify equal protein loading. (B) Extractions of the 9.4-kDa CP from SPMV/U-91-infected tissue were made in buffer (100 mM Tris-HCl, pH 7.5) (lane 1), buffer plus 1 M NaCl (lane 2), buffer plus 2% Triton X-100 (lane 3), or buffer plus 1% SDS (lane 4). In lane 4, the asterisk indicates an SPMV CP antibody-specific protein that was consistently observed.

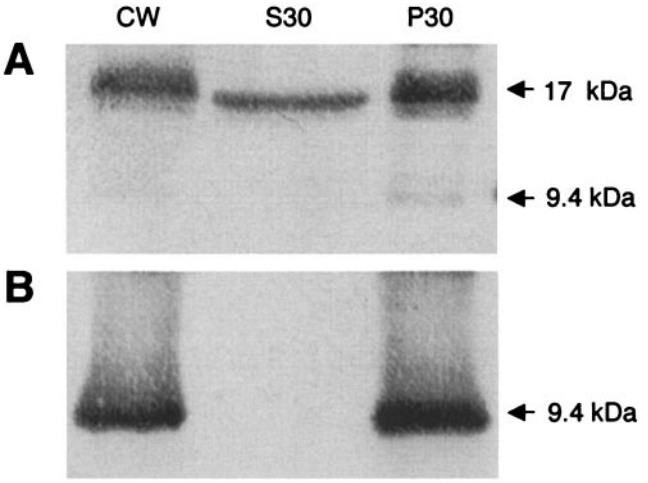

FIG. 3. Serological detection of SPMV CP in proso millet plants collected 14 days after inoculation of PMV plus SPMV or PMV plus SPMV/U-91 transcripts. The fractionation of cellular proteins by differential centrifugation is represented by CW (cell wall proteins), S30 (cytosolic proteins), and P30 (membranes). The proteins (indicated by arrows) were separated by SDS-PAGE and analyzed by Western blotting using SPMV CP-specific antiserum. (A) Plants infected with PMV and SPMV. (B) Plants infected with PMV and SPMV/U-91.

solution also significantly increased the amount of protein detection by Western blot assay. Interestingly, and similar to the full-length CP protein extraction, the addition of SDS resulted in immunodetection of a second slightly higher-molecular-weight protein, while Triton X-100 yielded a single protein band (Fig. 2B).

To study how differences in solubility might direct SPMV CP subcellular localization, we fractionated protein extracts from PMV- and SPMV-infected proso (Fig. 3) and foxtail millet plants by differential centrifugation. We found that a considerable amount of SPMV CP was localized to the cytosol, but the greatest accumulation was observed in membrane- and cell wall-associated fractions (Fig. 3A). Even more interestingly, the fractionation of extracts from plants infected with SPMV/U-91 (expressing the 9.4-kDa C-terminal version of CP) showed that the protein was exclusively associated with membrane-enriched and with cell wall-enriched fractions (Fig. 3B). Similar results were obtained for foxtail millet (not shown). These results suggest that cell wall and membrane cofractionation of SPMV CP is determined by the C-terminal portion of the protein. This would support a separate role for this region, which is in agreement with our finding that this truncated protein can be translated separately. The cofractionation of the capsid protein with the cell wall and membranes may indicate CP localization within these cell structures and designate protein involvement in systemic spread of the virus. To examine this possibility in some detail, we studied the effects of the protein expression on systemic accumulation of SPMV, as described in the following section.

Capsid protein facilitates SPMV RNA systemic accumulation in millet plants. Previously we reported that although SPMV CP deletion mutants were competent for replication and spread when coinfected with PMV, the titer was often greatly reduced (21). From this we made a series of N- and C-terminal CP derivatives to more closely evaluate the contribution of the capsid in SPMV RNA systemic accumulation. The construct SPMV/ΔBsmI-MscI has a deletion from nt 248 to 456, representing the majority of the C-terminal region of the CP open reading frame (Fig. 1A). Transcripts of this mutant were infectious, although the accumulation in the upper noninoculated leaves was host dependent (Fig. 4). Foxtail millet plants accumulated significantly less SPMV/ΔBsmI-MscI RNA compared to proso millet (Fig. 4A), yet the SPMV CP deletion did not have any profound effect on PMV accumulation (Fig. 4C). This suggested that expression of the full-length CP (or at least its C-terminal part) is essential for efficient SPMV systemic spread in foxtail plants.

To examine more precisely the effect of CP inactivation, we introduced a double frameshift mutation (SPMV/U-301) on the SPMV cDNA. This fully suppressed SPMV CP translation, as was evident when transcripts were assayed by in vitro translation in both wheat germ extract and rabbit reticulocyte lysate (data not shown). As predicted, the SPMV CP was not present in plants infected with PMV plus SPMV/U-301 (Fig. 5A). PMV RNA (not shown) and CP accumulation (Fig. 5A) were not affected by SPMV/U-301. SPMV/U-301 RNA was detected in the upper noninoculated leaves of proso and foxtail millet

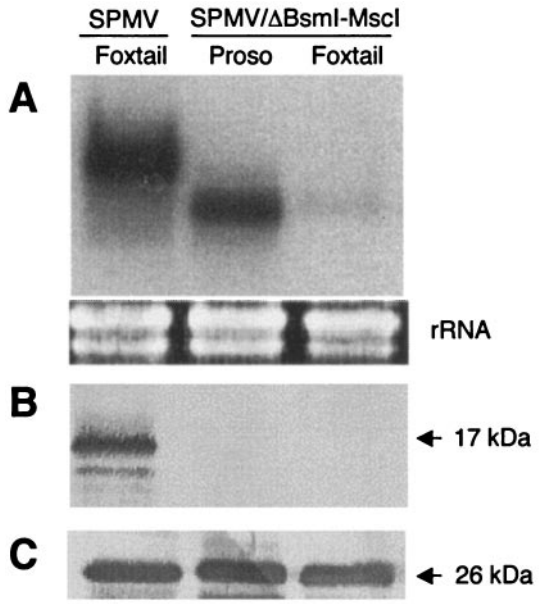

FIG. 4. Host-dependent movement of SPMV/ΔBsmI-MscI in millet following coinfection with PMV. (A) RNA was isolated from upper noninoculated leaves of infected foxtail and proso millet plants. The upper panel represents an RNA blot probed with ^{32}P-labeled SPMV. The lower panel represents an ethidium bromide-stained gel to verify equal loading of RNA, represented by rRNA, for each sample. (B and C) Western blots of SPMV CP (B) or PMV CP (C) isolated from upper leaves of infected millet plants. The expressed proteins are indicated by arrows.

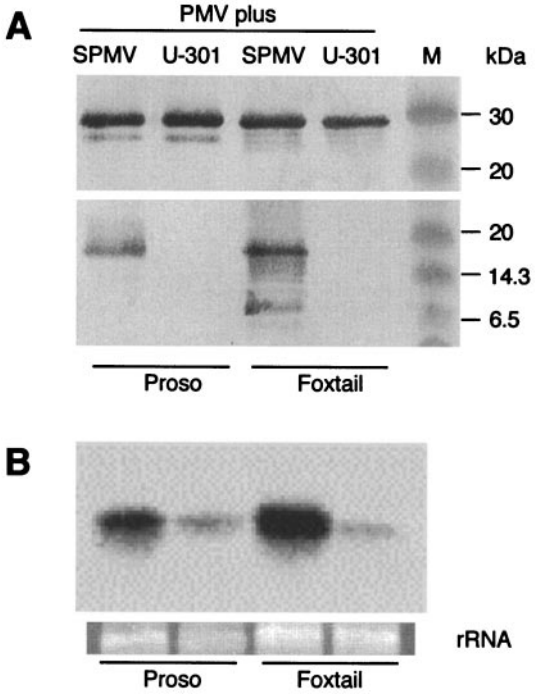

FIG. 5. SPMV RNA accumulation in upper noninoculated leaves with PMV plus SPMV/U-301. (A) Immunodetection of the 26-kDa PMV CP (upper panel) and the 17-kDa SPMV CP (lower panel) in upper uninoculated leaves of proso and foxtail millet plants 14 dpi with PMV plus wild-type SPMV or SPMV/U-301 (a double frameshift mutant to abolish CP expression). Molecular mass markers (in kilodaltons) are indicated on the rightmost side of the blot. (B) SPMV RNA accumulation as detected by Northern blotting using an SPMV-specific probe (upper panel). The lower panel is rRNA from an ethidium bromide-stained agarose gel, indicating equal loading for each sample.

plants but at lower levels than for SPMV wild-type infections (Fig. 5B). Interestingly, the amount of SPMV/U-301 RNA in the upper leaves was not host dependent, in contrast to the results for SPMV/ΔBsmI-MscI (Fig. 4).

The implications of these data are that the removal of portions of the SPMV RNA (as in Fig. 4) does not have a nonspecific beneficial effect on systemic accumulation of the virus, e.g., due to size-selective permeability of the plasmodesmata (compare results of proso millet in Fig. 4 and 5). Moreover, SPMV CP, especially the C-terminal portion, significantly enhanced systemic accumulation of SPMV RNA (Fig. 5), and this influence in conjunction with its RNA deletion is host specific (Fig. 4). This implies that the 9.4-kDa protein (either as a component of the full-length CP or as a separate unit) contributes in a host-dependent manner to virus spread.

SPMV CP contributes to systemic movement in foxtail plants in association with the SPMV 5′-UTR. It was found previously (21) that deletions from nt 67 to 104 (SP4) or nt 67 to 311 (SP5) on the SPMV genome did not affect systemic movement in proso millet plants, while the same mutations effectively impaired systemic movement of SPMV in foxtail plants. Since the deletions also removed the SPMV start codon at nt 88, translation of full-length SPMV CP was abolished. Thus, these circumstances raised the possibility of cooperative involvement of the SPMV CP and the 5′-UTR in systemic spread of SPMV RNA in foxtail millet plants. In order to examine this scenario, two sets of experiments were performed in parallel.

To ensure translation of the full-length version (17 kDa) of the CP, several mutants were constructed from the wild-type SPMV cDNA. A unique BamHI site, producing a silent mutation (20), was introduced at nt 78 on the 5′-UTR. This permitted access to a small region from SpeI and BamHI (nt 63 to 78) for further manipulations (Fig. 1A). The second set of mutants was constructed with SPMV-AUC, a construct that expresses an N-terminal-truncated version of SPMV CP (24). Then, as in case with wild-type SPMV, a BamHI site was created at nt 78. Both SPMV/ΔSpeI-BamHI, based on wild-type SPMV, and SPMV/AUC/ΔSpeI-BamHI (from SPMV/AUC) have a 15-nt deletion from SpeI to BamHI (Fig. 1A). An insertion of 4 nt by digestion with BamHI at position nt 78 followed by Klenow treatment also creates a ClaI restriction site on mutants SPMV/insertClaI (wild-type SPMV backbone) and SPMV/AUC/insertClaI from the SPMV/AUC construct. Proso and foxtail millet plants infected with the 5′-UTR deletion and insertion mutants expressing the full-length SPMV CP were indistinguishable from wild-type SPMV infections. This was concluded from comparison of SPMV RNA and capsid protein expression with RNA and immunoblot analyses, respectively (Fig. 6A).

The deletion of the N-terminal end of the SPMV CP resulted in reduced RNA accumulation (Fig. 6B). In Fig. 4, a similar effect is shown in the absence of the C-terminal portion of the CP, and in Fig. 5, when the expression of SPMV CP was

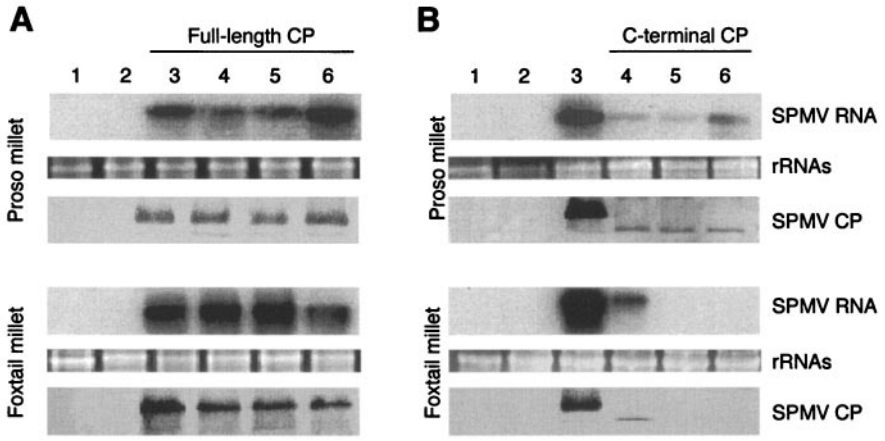

FIG. 6. SPMV RNA and CP accumulation from 5′-UTR mutants of SPMV and SPMV/AUC. The upper noninoculated leaves of proso and foxtail millet plants coinfected with PMV and the respective mutants were used for Western and Northern blotting. Equal loading of RNA was determined by visualizing rRNA levels on ethidium bromide-stained agarose gels, prior to transfer to membranes. For panels A and B, lanes 1, 2, and 3 represent mock, PMV, and PMV plus SPMV inoculations, respectively. (A) SPMV 5′-UTR derivatives that retain the expression of the full-length CP (lanes 4 to 6), representing mixed infections of PMV plus SPMV/BamHI, SPMV/ΔSpeI-BamHI, or SPMV/insertClaI, respectively. (B) SPMV/AUC-derived constructs that express the 9.4-kDa C-terminal CP. Lanes 4 to 6 represent mixed infections of PMV plus SPMV/AUC, SPMV/AUC/ΔSpeI-BamHI, or SPMV/AUC/insertClaI, respectively.

completely abolished, the RNA accumulation also was perturbed. The amount of viral RNA and truncated CP detected in upper leaves of proso millet plants infected with the SPMV/AUC-derived mutants (SPMV/AUC; SPMV/AUC/ΔSpeI-BamHI and SPMV/AUC/insertClaI) was significantly lower compared to plants inoculated with wild-type SPMV transcripts (Fig. 6B). In addition, we did observe a host-specific effect of the 5′-UTR modifications. For example, although the parental SPMV/AUC mutant (with an intact 5′-UTR) accumulated in the upper noninoculated leaves of foxtail millet, mutants containing 5′-UTR insertions and deletions (nt 63 to 78) did not accumulate systemically in this host (Fig. 6B).

Cumulatively, the data indicate that the capsid protein of SPMV facilitates systemic accumulation of SPMV in both proso and foxtail millet plants. However, the combination of CP truncation and the 5′-UTR modifications completely prohibited systemic accumulation of SPMV in foxtail millet plants.

SPMV CP specifically interacts with PMV CP. To examine interactions between the SPMV capsid protein and PMV-encoded proteins and to explore potential interactions with host proteins, we conducted pull-down experiments. For this purpose, in vivo [^{35}S]methionine protein labeling of healthy and PMV- and SPMV-infected plants was followed by immunoprecipitation with SPMV CP-specific antiserum. Extracts of PMV- and SPMV-infected proso millet leaf tissue subjected to this procedure yielded three proteins. Along with the expected 17-kDa capsid protein of SPMV, two other proteins with molecular masses of approximately 26 and 40 kDa were detected (Fig. 7A). The precipitation of the ~40-kDa protein is most likely due to a nonspecific reaction with SPMV CP antibody or the protein-G agarose complex, because this protein was also readily detectable in extracts of mock-inoculated (healthy) proso millet plants subjected to immunoprecipitation assay (Fig. 7A).

In extracts from proso millet plants infected with helper virus alone, the capsid protein of PMV was immunoprecipitated exclusively by PMV but not SPMV CP antiserum (Fig. 7B). The 26-kDa protein was detected in plants coinfected with PMV+SPMV, but not mock-inoculated plants. The molecular mass of the protein was identical to that of the capsid protein of helper virus (PMV). To confirm this, extracts of PMV- and SPMV-infected proso millet leaves were subjected to immunoprecipitation using, separately, SPMV CP and PMV CP antiserum. The immunoprecipitated material was then cross-analyzed by Western blotting with SPMV CP or PMV CP antiserum as a probe. Our results show that pull-downs with SPMV CP antibody coprecipitated PMV CP (Fig. 7C) and vice versa: immunoprecipitation with PMV CP antiserum also revealed a cointeraction with SPMV CP after Western blot analysis (Fig. 7D). These data clearly show that a stable interaction occurs between PMV capsid protein and the satellite virus CP. This offers the possibility that the host-dependent effect of SPMV CP on movement may be partially related to its interaction with PMV CP.

DISCUSSION

Initiation of translation in eukaryotes is regulated by several factors, including mRNA length, the 5′-UTR, secondary structure, and the nucleotide context surrounding AUG start codons (7, 11, 13, 17, 32). Eukaryotic mRNAs generally adhere to the first AUG rule—in most cases, the AUG codon nearest the 5′ end is the sole site of initiation of translation (13). However, if the first AUG codon is positioned in a suboptimal context, initiation may also occur from the second AUG codon, producing two proteins (14). Both cellular and viral mRNAs have been reported to produce two separately initiated proteins by context-dependent leaky scanning (15). Our results show that the SPMV CP gene directs protein translation from the first (AUG1) and third (AUG3) start codons, both of which are in the same translational frame. The nucleotide sequence surrounding AUG1 (CUCCUGAUGG) is sub-

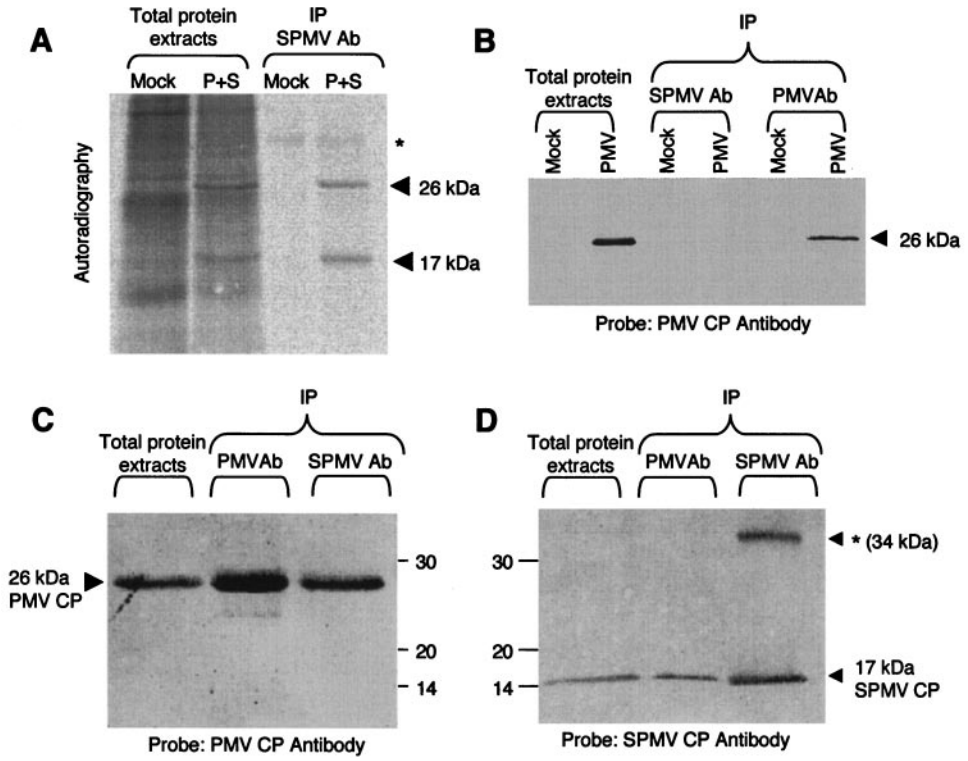

FIG. 7. Biomolecular interactions between PMV and SPMV capsid proteins. (A) Healthy (mock) and PMV- and SPMV-infected (P+S) proso millet plants were labeled in planta with [^{35}S]methionine. The left panel shows total protein extracts, and the right panel is an autoradiograph after a pull-down assay using SPMV CP-specific antiserum for immunoprecipitation (IP). The asterisk indicates the position of a host protein (in healthy and infected plants). The PMV (26-kDa) and SPMV (17-kDa) capsid proteins are indicated with arrows. (B) Immunoprecipitation and detection of PMV CP from extracts of infected proso millet leaves. PMV-inoculated plants were subjected to immunoprecipitation, as separate assays, with SPMV CP or PMV CP antiserum. The resultant precipitate was eluted, subjected to Western blotting, and analyzed for the presence of PMV CP using PMV CP antibody as a probe. (C and D) Coimmunoprecipitation of SPMV and PMV capsid proteins from extracts of infected proso millet leaves. PMV- and SPMV-infected plants were subjected to immunoprecipitation using antiserum specific for either SPMV CP or PMV CP. The immunoprecipitates were eluted and separately subjected to Western blotting and probed with polyclonal antiserum specific for PMV CP (C) or SPMV CP (D). The asterisk indicates the position of the dimeric form of SPMV CP (~34 kDa). The arrowheads show positions and molecular masses of precipitated proteins.

optimal; the optimal sequence context for translational initiation is GCCRCCAUGG (R is a purine).

Our experimental results suggest that G-rich regions immediately upstream and downstream of the AUG2 may prompt the ribosome to scan to AUG3. This was the case in planta, although the AUG2-encoded protein was weakly translated in vitro. The C-terminal portion of the SPMV CP is associated with a severe symptom phenotype in infected millet plants (24). Supportively, the results of this study revealed that the absence of 9.4-kDa C-terminal product expression in the case of the SPMV/UAA-234 mutant resulted in mild mosaic on millet plants compared to severe symptoms caused by SPMV wild type and SPMV/U-91, which are both associated with C-terminal protein expression. This may further indicate a separate role of the 9.4-kDa truncated CP product in SPMV-associated symptom modulation. Moreover, this phenomenon may be an effect of the biochemical properties of the C-terminal portion of SPMV CP, in that the 9.4-kDa protein associated exclusively with the cell wall- and membrane-enriched fractions of PMV+SPMV-infected millet plants. Perturbation of host membranes may play a pivotal role in the mechanism of severe symptoms induction associated with PMV and SPMV, compared to the very mild mosaic associated with PMV infection alone. More detailed studies on protein subcellular localization are necessary to pinpoint the precise mechanism of the SPMV CP-mediated symptom modulation on millet host plants.

Recently it was shown that a satellite virus of *Macrobrachium rosenbergii*, a nodavirus that infects freshwater prawns, translates two proteins, a 17-kDa CP and an N-terminal-truncated 16-kDa protein (36), from its plus-sense single-stranded RNA genome. Although the biological significance of this phenomenon remains unclear, Widada and Bonami (36) noted that the N-terminal domain of all satellite virus capsid proteins have a common motif containing hydrophilic amino acids and a positively charged arginine. This observation, along with data presented in the current work, suggests that the N-terminal domain of CP facilitates protein solubility, and as a result it is localized to the cytoplasm, where virions are assembled.

In addition to virion assembly, capsid proteins may contribute to other virus-related biological activities, including replication, symptom modulation, cell-to-cell movement, and systemic spread (4, 10, 35). For example, the *Brome mosaic virus* CP is essential for systemic and cell-to-cell movement, and this

requirement is host specific (9, 20, 27). The very closely related *Cowpea chlorotic mottle virus* capsid protein is not required for cell-to-cell movement (26). However, *Cowpea chlorotic mottle virus* CP is essential for systemic spread (1), although virion formation is not (28). Rod-shaped viruses such as *Potato virus X* (5) and *Beet necrotic yellow vein virus* (25) also require functional CP for systemic movement in plants.

The data presented in this paper demonstrate that SPMV capsid protein facilitates systemic spread of this satellite virus. The suppression of CP translation, with frameshift and deletion mutants, significantly decreased the accumulation of SPMV RNA in upper, noninoculated leaves of plants. Moreover, the results of this study also show that SPMV CP in association with a small portion of the 5′-UTR facilitates systemic SPMV RNA accumulation in a host-specific manner. The subcellular cofractionation of SPMV CP to membrane- and cell wall-enriched fractions suggests a functional involvement as a movement-associated protein in systemic spread of the satellite virus.

It remains to be resolved why in foxtail millet the expression of the N-terminal domain of SPMV CP compensated for deletions or insertions of nucleotides in the 5′-UTR, while in proso millet the same mutations did not impair SPMV systemic spread regardless of the presence of CP. Interaction with viral RNA is another characteristic biochemical feature associated with movement proteins of plant viruses (12), one that we have also reported for SPMV CP (6). Perhaps systemic spread of SPMV in foxtail millet requires an interaction between the 5′-UTR and N-terminal region of the capsid protein. In contrast, the lack of such an interaction in proso millet may be provided by as-yet-unidentified host, biochemical, and/or physiological factors.

Alternatively (or in addition), the compensatory effect of CP on SPMV systemic translocation in foxtail millet may involve a specific CP interaction with the capsid protein of the helper virus (PMV), while such interaction is not essential for systemic movement in proso plants. In support of this hypothesis is our observation that coprecipitation of PMV capsid protein using SPMV CP antiserum was detected exclusively when full-length SPMV CP was expressed in infected plants (not shown). The absence of interaction between the 9.4-kDa truncated SPMV CP and the PMV CP may lead to explanations for the decreased amount of SPMV RNA accumulation in upper leaves of proso and foxtail millet infected with SPMV/AUC mutants versus wild type (Fig. 6). The wild-type CP may also protect the RNA from degradation via efficient RNA packaging and virion formation. Overall, the mechanism of host-specific systemic spread of SPMV likely involves a complex cross-specific interaction between SPMV RNA, host factors, and movement proteins of the helper virus. SPMV RNA may direct synthesis of N-terminal-truncated proteins as accessory factors to enhance SPMV infectivity, including replication and movement, by directing the RNA to the cell wall and membranes.

In summary, our results indicate that multifunctional features of SPMV CP are essential to sustain its robustness when supported by a PMV infection in a host plant. The specific associations between PMV and SPMV capsid proteins suggest that important molecular interactions occur between the satellite virus and helper virus in the plant. It is noteworthy to mention here that the previously documented pattern of subcellular localization of PMV CP (33) is strikingly similar to results presented here on fractionation of SPMV CP at subcellular level. Interestingly, a recent study showed that contaminating virions of SPMV are incorporated into PMV crystals by insertion into the interstices between PMV virions in the crystal lattice (18). Is colocalization of PMV CP and SPMV CP important for SPMV (and PMV) movement? At the very least SPMV RNA must be in proximity to the PMV replicase proteins; perhaps the SPMV CP acts as a guide for intracellular localization.

ACKNOWLEDGMENTS

This work was funded by USDA-NRI (99-3503-7974) and THECB-ATP (000517-0043-2003) grants awarded to K.-B.G. Scholthof.

We thank Herman Scholthof for his valuable comments and critical review of the manuscript.

REFERENCES

1. **Allison, R., C. Thompson, and P. Ahlquist.** 1990. Regeneration of a functional RNA virus genome by recombination between deletion mutants and requirement for cowpea chlorotic mottle virus 3a and coat genes for systemic infection. Proc. Natl. Acad. Sci. USA **87:**1820–1824.
2. **Batten, J. S.** 2002. Replication and translation of panicum mosaic virus. Ph.D. dissertation. Texas A&M University, College Station.
3. **Buzen, F. G., C. L. Niblett, G. R. Hooper, J. Hubbard, and M. A. Newman.** 1984. Further characterization of panicum mosaic virus and its associated satellite virus. Phytopathology **74:**313–318.
4. **Callaway, A., D. Giesman-Cookmeyer, E. T. Gillock, T. L. Sit, and S. A. Lommel.** 2001. The multifunctional capsid proteins of plant RNA viruses. Annu. Rev. Phytopathol. **39:**419–460.
5. **Chapman, S., T. Kavanagh, and D. Baulcombe.** 1992. Potato virus X as a vector for gene expression in plants. Plant J. **2:**549–557.
6. **Desvoyes, B., and K.-B. G. Scholthof.** 2000. RNA:protein interactions associated with satellites of panicum mosaic virus. FEBS Lett. **485:**25–28.
7. **Dinesh-Kumar, S. P., and W. A. Miller.** 1993. Control of start codon choice on a plant viral RNA encoding overlapping genes. Plant Cell **5:**679–692.
8. **Dodds, J. A.** 1998. Satellite tobacco mosaic virus. Annu. Rev. Phytopathol. **36:**295–310.
9. **Flasinski, S., A. Dzianott, S. Pratt, and J. J. Bujarski.** 1995. Mutational analysis of the coat protein gene of brome mosaic virus: effects on replication and movement in barley and in *Chenopodium hybridum*. Mol. Plant-Microbe Interact. **8:**23–31.
10. **Guogas, L. M., D. J. Filman, J. M. Hogle, and L. Gehrke.** 2004. Cofolding organizes alfalfa mosaic virus RNA and coat protein for replication. Science **306:**2108–2111.
11. **Hinton, T. M., F. Li, and B. S. Crabb.** 2000. Internal ribosomal entry site-mediated translation initiation in equine rhinitis A virus: similarities to and differences from that of foot-and-mouth disease virus. J. Virol. **74:**11708–11716.
12. **Ivanov, K. I., P. Puustinen, R. Gabrenaite, H. Vihinen, L. Ronnstrand, L. Valmu, N. Kalkkinen, and K. Makinen.** 2003. Phosphorylation of the potyvirus capsid protein by protein kinase CK2 and its relevance for virus infection. Plant Cell **15:**2124–2139.
13. **Kozak, M.** 1995. Adherence to the first-AUG rule when a second AUG codon follows closely upon the first. Proc. Natl. Acad. Sci. USA **92:**2662–2666.
14. **Kozak, M.** 1996. Interpreting cDNA sequences: some insights from studies on translation. Mamm. Genome **7:**563–574.
15. **Kozak, M.** 2002. Pushing the limits of the scanning mechanism for initiation of translation. Gene **299:**1–34.
16. **Langstein, J., and H. Schwarz.** 1997. Suppression of irrelevant signals in immunoblots by preconjugation of primary antibodies. BioTechniques **23:**1006–1008.
17. **Liu, J., G. Prolla, A. Rostagno, R. Chiarle, H. Feiner, and G. Inghirami.** 2000. Initiation of translation from a downstream in-frame AUG codon on BRCA1 can generate the novel isoform protein DeltaBRCA1(17aa). Oncogene **19:**2767–2773.
18. **Makino, D. L., S. B. Larson, and A. McPherson.** 2005. Preliminary analysis of crystals of panicum mosaic virus (PMV) by X-ray diffraction and atomic force microscopy. Acta Crystallogr. D **61:**173–179.
19. **Masuta, C., D. Zuidema, B. G. Hunter, L. A. Heaton, D. S. Sopher, and A. O. Jackson.** 1987. Analysis of the genome of satellite panicum mosaic virus. Virology **159:**329–338.
20. **Okinaka, Y., K. Mise, E. Suzuki, T. Okuno, and I. Furusawa.** 2001. The C terminus of brome mosaic virus coat protein controls viral cell-to-cell and long-distance movement. J. Virol. **75:**5385–5390.

21. **Qiu, W., and K.-B. G. Scholthof.** 2000. In vitro- and in vivo-generated defective RNAs of satellite panicum mosaic virus define *cis*-acting RNA elements required for replication and movement. J. Virol. **74:**2247–2254.
22. **Qiu, W., and K.-B. G. Scholthof.** 2004. Satellite panicum mosaic virus capsid protein elicits symptoms on a nonhost plant and interferes with a suppressor of virus-induced gene silencing. Mol. Plant-Microbe Interact. **17:**263–271.
23. **Qiu, W. P., and K.-B. G. Scholthof.** 2001. Defective interfering RNAs of a satellite virus. J. Virol. **75:**5429–5432.
24. **Qiu, W. P., and K.-B. G. Scholthof.** 2001. Genetic identification of multiple biological roles associated with the capsid protein of satellite panicum mosaic virus. Mol. Plant-Microbe Interact. **14:**21–30.
25. **Quillet, L., H. Guilley, G. Jonard, and K. Richards.** 1989. In vitro synthesis of biologically active beet necrotic yellow vein virus RNA. Virology **172:**293–301.
26. **Rao, A. L.** 1997. Molecular studies on bromovirus capsid protein. III. Analysis of cell-to-cell movement competence of coat protein defective variants of cowpea chlorotic mottle virus. Virology **232:**385–395.
27. **Schmitz, I., and A. L. N. Rao.** 1996. Molecular studies on bromovirus capsid protein I. Characterization of cell-to-cell movement-defective RNA3 variants of brome mosaic virus. Virology **226:**281–293.
28. **Schneider, W. L., A. E. Greene, and R. F. Allison.** 1997. The carboxy-terminal two-thirds of the cowpea chlorotic mottle bromovirus capsid protein is incapable of virion formation yet supports systemic movement. J. Virol. **71:**4862–4865.
29. **Scholthof, K.-B. G.** 1999. A synergism induced by satellite panicum mosaic virus. Mol. Plant-Microbe Interact. **12:**163–166.
30. **Scholthof, K.-B. G., R. W. Jones, and A. O. Jackson.** 1999. Biology and structure of plant satellite viruses activated by icosahedral helper viruses. Curr. Top. Microbiol. Immunol. **239:**123–143.
31. **Simon, A. E., M. J. Roossinck, and Z. Havelda.** 2004. Plant virus satellite and defective interfering RNAs: new paradigms for a new century. Annu. Rev. Phytopathol. **42:**415–437.
32. **Slusher, L. B., E. C. Gillman, N. C. Martin, and A. K. Hopper.** 1991. mRNA leader length and initiation codon context determine alternative AUG selection for the yeast gene MOD5. Proc. Natl. Acad. Sci. USA **88:**9789–9793.
33. **Turina, M., B. Desvoyes, and K.-B. G. Scholthof.** 2000. A gene cluster encoded by panicum mosaic virus is associated with virus movement. Virology **266:**120–128.
34. **Turina, M., M. Maruoka, J. Monis, A. O. Jackson, and K.-B. G. Scholthof.** 1998. Nucleotide sequence and infectivity of a full-length cDNA clone of panicum mosaic virus. Virology **241:**141–155.
35. **Vaewhongs, A. A., and S. A. Lommel.** 1995. Virion formation is required for the long-distance movement of red clover necrotic mosaic virus in movement protein transgenic plants. Virology **212:**607–613.
36. **Widada, J. S., and J. R. Bonami.** 2004. Characteristics of the monocistronic genome of extra small virus, a virus-like particle associated with *Macrobrachium rosenbergii* nodavirus: possible candidate for a new species of satellite virus. J. Gen. Virol. **85:**643–646.